

## OXYGEN OVERABUNDANCE IN THE EXTREMELY IRON-POOR STAR CS 29498-043<sup>1</sup>

WAKO AOKI,<sup>2</sup> JOHN E. NORRIS,<sup>3</sup> SEAN G. RYAN,<sup>4</sup> TIMOTHY C. BEERS,<sup>5</sup> NORBERT CHRISTLIEB,<sup>6</sup>  
STELIOS TSANGARIDES,<sup>4</sup> AND HIROYASU ANDO<sup>2</sup>

Received 2003 October 17; accepted 2004 February 26

### ABSTRACT

An abundance analysis for the carbon-enhanced, extremely iron-poor ( $[\text{Fe}/\text{H}] \sim -3.5$ ) star CS 29498-043 has been obtained using new high-resolution, high signal-to-noise ratio spectra from the Subaru Telescope. The  $[\text{O I}]$  forbidden line at 6300 Å and the O I triplet feature at 7771–7776 Å are both clearly detected. The overabundance of oxygen is significant ( $[\text{O}/\text{Fe}] > 2$ ). In addition, Na, Co, and Ni abundances have been newly measured. The abundance pattern from C to Ni of this object is quite similar to that of CS 22949-037, another extremely metal-poor star with large excesses of C, N, O, and the  $\alpha$ -elements. The abundance patterns of these two stars suggest the existence of supernovae progenitors that ejected relatively little material from their iron cores during the very early era of nucleosynthesis in the Galaxy. The metallicity in these objects, when one includes the elements C, N, and O in the tally of total metals, is not as low as in the most metal-poor stars, suggesting the existence of quite different formation processes for these iron-deficient objects than pertain to the bulk of other metal-deficient stars.

*Subject headings:* nuclear reactions, nucleosynthesis, abundances — stars: abundances — stars: carbon — stars: individual (CS 29498-043) — stars: Population II

*On-line material:* machine-readable table

### 1. INTRODUCTION

The surface chemical composition of extremely metal-poor stars is believed to reflect the yields of heavy elements produced by the first generations of massive stars in our Galaxy. Reported large variations of the elemental abundance patterns of some species (in particular those associated with carbon and the neutron-capture elements) found in very metal-poor stars (e.g., McWilliam et al. 1995; Ryan et al. 1996; Cayrel et al. 2004) suggest a diversity of the nucleosynthesis and explosion mechanisms of the supernovae that were presumably responsible.

Our previous study of the extremely metal-poor star CS 29498-043 ( $[\text{Fe}/\text{H}] \sim -3.7$ ) revealed remarkable overabundances of C, N, Mg, and Si in this object (Aoki et al. 2002a, 2002b).<sup>7</sup> The chemical nature of this object, which is similar to another extremely metal-poor star, CS 22949-037 (McWilliam et al. 1995; Norris et al. 2001; Depagne et al. 2002), suggests that these objects formed from the yields of supernovae that ejected relatively little material from the regions surrounding their iron cores at the time of their explosion (e.g., Tsujimoto & Shigeyama 2003; Umeda & Nomoto 2003). A remaining important question is the origin

of the large overabundances of C and N, because these two elements are expected to be significantly affected during the evolution of low-mass stars. In order to distinguish the contributions of low- and high-mass stars, determinations of the O abundance, as well as those of the  $\alpha$ -elements, are quite important. The O abundance is also vital to estimate the metallicity of this object. In this paper, we report a new analysis of the chemical composition of CS 29498-043, including the O abundance, derived from high-resolution, high signal-to-noise ratio spectra obtained with the Subaru Telescope.

### 2. OBSERVATIONS AND MEASUREMENTS

The observations reported here were obtained with the Subaru Telescope High Dispersion Spectrograph (HDS; Noguchi et al. 2002), with a spectral resolving power  $R = 50,000$ , in 2002 October and 2003 May. The wavelength coverage and signal-to-noise ratios (S/N) per pixel are listed in Table 1. The EEV CCD with 13.5  $\mu\text{m}$  pixels was used with the  $2 \times 2$  binning mode. Standard data-reduction procedures were carried out with the IRAF echelle package.<sup>8</sup>

For the abundance analysis described herein, we combined these spectra with a similar quality blue spectrum obtained in our previous study (Aoki et al. 2002a). Equivalent widths of absorption lines for 12 metals (14 ionization species) were measured by fitting Gaussian profiles and are listed in Table 2 along with the line data used in the analysis.

In order to investigate the binarity of this object, which might have relevance for the interpretation of the origin of the abundance peculiarities, we measured heliocentric radial velocities ( $V_r$ ) for each spectrum, as given in Table 1. The measurements were made using clean, isolated Fe I lines. Our measurements for spectra obtained in previous observing runs

<sup>1</sup> Based on data collected at the Subaru Telescope, which is operated by the National Astronomical Observatory of Japan.

<sup>2</sup> National Astronomical Observatory, Mitaka, 181-8588 Tokyo, Japan; aoki.wako@nao.ac.jp, ando@optik.mtk.nao.ac.jp.

<sup>3</sup> Research School of Astronomy and Astrophysics, The Australian National University, Mount Stromlo Observatory, Cotter Road, Weston, ACT 2611, Australia; jen@mso.anu.edu.au.

<sup>4</sup> Department of Physics and Astronomy, The Open University, Walton Hall, Milton Keynes, MK7 6AA, UK; s.g.ryan@open.ac.uk, s.tsangarides@open.ac.uk.

<sup>5</sup> Department of Physics and Astronomy, Michigan State University, East Lansing, MI 48824-1116; beers@pa.msu.edu.

<sup>6</sup> Hamburger Sternwarte, Universität Hamburg, Gojenbergsweg 112, D-21029 Hamburg, Germany; nchristlieb@hs.uni-hamburg.de.

<sup>7</sup>  $[A/B] = \log(N_A/N_B) - \log(N_A/N_B)_\odot$ , and  $\log \epsilon_A = \log(N_A/N_H) + 12$  for elements A and B.

<sup>8</sup> IRAF is distributed by the National Optical Astronomy Observatory, which is operated by the Association of Universities for Research in Astronomy, Inc., under cooperative agreement with the National Science Foundation.

TABLE 1  
SUBARU OBSERVATIONS FOR CS 29498-043

Observation Date (JD)	Wavelength (Å)	Exposure (min)	S/N <sup>a</sup>	Radial Velocity (km s <sup>-1</sup> )
2000 Sep (2,451,802) <sup>b</sup> .....	3770–4760	270	45	-32.50 ± 0.18
2001 Jul (2,452,115) <sup>c</sup> .....	3550–5250	120	87	-32.60 ± 0.46
2002 Oct (2,452,573).....	5100–7800	80	112	-32.74 ± 0.42
2003 May (2,452,785).....	5100–7800	90	148	-32.95 ± 0.39
2003 May (2,452,786).....	3550–5250	90	77	-33.10 ± 0.45

<sup>a</sup> S/N ratios are 1.8 km s<sup>-1</sup> pixel<sup>-1</sup> at 4320 and 6270 Å for the blue and red spectra, respectively.

<sup>b</sup> Based on spectra obtained with Anglo-Australian Telescope (AAT) UCLES.

<sup>c</sup> Results of this observing run have already been reported in Aoki et al. (2002a, 2002b).

are also given in Table 1. No clear variation of the radial velocities is found for this object, although the  $V_r$  values are slightly decreasing over the past 3 years. Further monitoring of radial velocity to determine if it is in fact a long-period binary is clearly desirable.

### 3. ANALYSIS AND RESULTS

An LTE abundance analysis was carried out using the model atmospheres of Kurucz (1993). An estimate of the effective temperature,  $T_{\text{eff}} = 4570$  K, was obtained from the  $V-K$  color index, using the Alonso et al. (1999) empirical temperature scale, adopting the photometry data from Norris et al. (1999) ( $V = 13.72$ ) and from the 2 Micron All Sky Survey Point Source Catalog (Skrutskie et al. 1997) ( $K = 10.94$ ), along with an interstellar reddening of  $E(B-V) = 0.09$ , estimated from the Schlegel et al. (1998) map. We adopted  $T_{\text{eff}} = 4600$  K for the following abundance analysis.

After the analysis was completed,  $R$  and  $I$  photometry data also became available, obtained with the ESO Danish 1.54 m telescope and the Danish Faint Object Spectrograph and Camera (DFOSC). The derived colors,  $V-R = 0.615$  and  $V-I = 1.222$  (Cousins system), result in temperature estimates of  $T_{\text{eff}} = 4570$  and 4500 K, respectively, if the Alonso et al. (1999) scale is applied. These results support our effective temperature determined from the  $V-K$  color.

In our previous analysis (Aoki et al. 2002a, 2002b), we adopted  $T_{\text{eff}} = 4400$  K as a preferred value, taking account of the correlation between the derived Fe abundances and the lower excitation potential of Fe I lines found in the result for  $T_{\text{eff}} = 4600$  K. However, this correlation is not clear in the present analysis, which includes new Fe I lines detected in the revised spectrum covering both blue and red ranges, especially the lines with high excitation potentials ( $\sim 4.3$  eV). For this reason, we have adopted  $T_{\text{eff}} = 4600$  K as the preferred value but consider 4400 K as an alternative choice.

Using the model atmospheres of Kurucz (1993) for the adopted effective temperatures, we performed abundance analyses in the standard manner for the measured equivalent widths. Surface gravities ( $\log g$ ) were determined from the ionization balance between Fe I and Fe II; the microturbulence ( $v_{\text{tur}}$ ) was determined from the Fe I lines by demanding no dependence of the derived abundance on equivalent widths. The effect of large enhancements of C, N, Mg, and Si were included in the calculation of chemical equilibrium for the abundance analysis. The excess of oxygen found in the present analysis, as noted below, was also taken into account. We note that these effects are not included in the calculations of the thermal structure of atmospheres, but they are estimated to be small for such low-metallicity stars. The final derived

atmospheric parameters are  $\log g = 1.2$ ,  $v_{\text{tur}} = 2.4$  km s<sup>-1</sup>, and  $[\text{Fe}/\text{H}] = -3.5$ .

The derived abundances ( $[\text{X}/\text{Fe}]$  and  $[\text{Fe}/\text{H}]$ ) are listed in Table 3. Column (6) provides the results when  $T_{\text{eff}} = 4400$  K is adopted. The surface gravity, determined by the same methods, but for  $T_{\text{eff}} = 4400$  K, is  $\log g = 0.6$ . We used the same microturbulence and metallicity as for  $T_{\text{eff}} = 4600$  K. For comparison, in column (7), we also provide the chemical abundances derived for the atmospheric parameters adopted by Israelian et al. (2004a, 2004b) ( $T_{\text{eff}} = 4300$  K,  $\log g = 1.5$ , and  $[\text{Fe}/\text{H}] = -3.5$ ). Since the iron abundances from Fe I and Fe II derived by our (LTE) analysis show a significant discrepancy (0.5 dex), we assumed  $[\text{Fe}/\text{H}] = -3.5$ , which is similar to the value derived from Fe II lines, to derive  $[\text{X}/\text{Fe}]$  values for individual elements.

#### 3.1. Oxygen

The [O I] 6300 Å line is clearly detected in the spectrum of CS 29498-043. Since at this wavelength the 2002 October spectrum is significantly affected by strong [O I] emission in the Earth's atmosphere, the analysis was made using the 2003 May spectrum, which provided a more favorable velocity shift. Figure 1a shows a comparison of the spectra of CS 29498-043 and a standard star (HD 178840) observed just after the observation of CS 29498-043 with a similar zenith distance. We confirmed that the telluric lines are corrected by the spectrum of the standard star within 1% of the continuum level for the lines at 6295.9, 6298.4, and 6302.0 Å. This indicates that telluric absorption does not significantly affect the measurement of the equivalent width of the [O I] line, which is estimated to be 31.4 mÅ (Table 2). The spectrum of this star, corrected for the telluric absorption lines (primarily H<sub>2</sub>O) and the Doppler shift estimated from clean Fe I lines, is shown as the dots in Figure 1b. The lines are synthetic spectra for the three assumed oxygen abundances presented in the figure.<sup>9</sup>

The equivalent width of the [O I] 6363 Å line measured for our spectrum is 14 mÅ, which provides a consistent oxygen abundance with that obtained from the [O I] 6300 Å line. However, the quality of the observed spectrum at 6363 Å is not as good as that at 6300 Å, and a few unidentified lines with similar strengths to the [O I] 6363 Å line appear around this wavelength. Therefore, we adopt the result obtained from the [O I] 6300 Å line for the oxygen abundance derived from forbidden lines.

<sup>9</sup> We adopt a solar oxygen abundance of  $\log \epsilon(\text{O})_{\odot} = 8.74$  determined from the 6300 Å forbidden line by Nissen et al. (2002), which is consistent with Allende Prieto et al. (2001) within the uncertainty.

TABLE 2  
EQUIVALENT WIDTHS

$\lambda$ (Å)	$\log gf$	$\chi$ (eV)	$W^a$ (mÅ)
O I			
6300.30.....	-9.820	0.000	31.4s
6363.78.....	-10.303	0.020	14.0x
7771.95.....	0.358	9.147	19.5s
7774.18.....	0.212	9.147	15.6s
7775.40.....	-0.010	9.147	10.9s
Na I			
5889.95.....	0.101	0.000	204.5
5895.92.....	-0.197	0.000	180.8
Mg I			
4057.50.....	-0.890	4.346	65.0
4571.10.....	-5.688	0.000	109.9
4702.99.....	-0.520	4.346	101.1
5172.69.....	-0.380	2.712	232.9x
5183.60.....	-0.160	2.717	253.4x
5528.40.....	-0.490	4.346	102.8
Al I			
3961.52.....	-0.340	0.010	136.5s
Si I			
4102.94.....	-2.910	1.909	75.5
Ca I			
5588.76.....	0.358	2.526	12.5
6102.72.....	-0.770	1.879	5.9
6122.22.....	-0.320	1.886	21.4
Sc II			
5526.79.....	0.020	1.768	6.0
Ti I			
4991.07.....	0.436	0.836	17.5
5173.74.....	-1.062	0.000	10.0
5210.38.....	-0.828	0.048	12.4
Ti II			
4468.52.....	-0.600	1.131	90.9
4501.27.....	-0.760	1.116	73.9
4533.97.....	-0.770	1.237	92.4
4563.77.....	-0.960	1.221	64.4
4571.96.....	-0.530	1.572	87.1
5185.90.....	-1.350	1.893	8.3
5188.69.....	-1.210	1.582	30.0
5226.53.....	-1.300	1.566	26.5
5381.01.....	-1.970	1.566	5.6
Cr I			
5208.44.....	0.158	0.941	54.2
5409.79.....	-0.720	1.030	8.9
Mn I			
4030.75.....	-0.470	0.000	83.7s
4033.07.....	-0.620	0.000	68.3s

TABLE 2—Continued

$\lambda$ (Å)	$\log gf$	$\chi$ (eV)	$W^a$ (mÅ)
Fe I			
4005.24.....	-0.610	1.557	92.5
4063.59.....	0.060	1.557	116.9
4071.74.....	-0.022	1.608	112.4
4461.65.....	-3.210	0.087	86.3
4466.55.....	-0.600	2.832	33.1
4489.74.....	-3.966	0.121	40.8
4494.56.....	-1.136	2.198	36.8
4528.61.....	-0.822	2.176	59.3
4531.15.....	-2.155	1.485	35.3
4592.65.....	-2.449	1.557	14.9
4602.94.....	-2.210	1.485	37.0
4871.32.....	-0.360	2.865	42.0
4890.75.....	-0.390	2.876	30.5
4891.49.....	-0.110	2.851	48.0
4903.31.....	-0.930	2.882	10.0
4918.99.....	-0.340	2.865	33.9
4920.50.....	0.070	2.833	56.0
4994.13.....	-2.956	0.915	26.6
5006.12.....	-0.610	2.833	23.1
5012.07.....	-2.642	0.859	61.5
5041.07.....	-3.090	0.958	28.6
5041.76.....	-2.200	1.485	34.3
5049.82.....	-1.344	2.279	26.3
5051.63.....	-2.795	0.915	46.3
5068.77.....	-1.040	2.940	11.5
5083.34.....	-2.958	0.958	38.6
5110.41.....	-3.760	0.000	61.5
5123.72.....	-3.068	1.011	31.7
5127.36.....	-3.307	0.915	22.4
5151.91.....	-3.322	1.011	24.8
5166.28.....	-4.195	0.000	38.5
5171.60.....	-1.793	1.485	55.1
5191.46.....	-0.550	3.038	15.3
5192.34.....	-0.420	2.998	22.5
5194.94.....	-2.090	1.557	36.6
5202.34.....	-1.838	2.176	14.2
5216.27.....	-2.150	1.608	30.8
5232.94.....	-0.060	2.940	43.0
5254.96.....	-4.764	0.110	10.7
5266.56.....	-0.390	2.998	24.6
5269.54.....	-1.321	0.859	129.7
5328.04.....	-1.466	0.915	122.2
5328.53.....	-1.850	1.557	52.7
5332.90.....	-2.780	1.557	10.7
5341.02.....	-1.950	1.608	38.9
5369.96.....	0.540	4.371	9.0
5371.49.....	-1.645	0.958	111.5
5383.37.....	0.640	4.312	9.7
5397.13.....	-1.993	0.915	99.6
5405.77.....	-1.844	0.990	99.9
5415.20.....	0.640	4.386	8.9
5424.07.....	0.520	4.320	14.6
5429.70.....	-1.879	0.958	101.0
5434.52.....	-2.122	1.011	80.8
5446.92.....	-1.910	0.990	95.2
5455.61.....	-2.098	1.011	92.9
5497.52.....	-2.849	1.011	39.3
5506.78.....	-2.797	0.990	43.3
5572.84.....	-0.275	3.397	17.2
5586.75.....	-0.096	3.368	21.0
5615.64.....	0.050	3.332	24.4
6065.48.....	-1.530	2.609	11.4

TABLE 2—Continued

$\lambda$ (Å)	$\log gf$	$\chi$ (eV)	$W^a$ (mÅ)
6136.61.....	-1.400	2.453	18.9
6230.72.....	-1.281	2.559	17.1
6393.60.....	-1.432	2.433	20.2
Fe II			
4508.28.....	-2.580	2.856	11.8
4520.23.....	-2.600	2.807	6.2
4583.83.....	-2.020	2.807	30.1
4923.93.....	-1.320	2.891	51.2
5018.45.....	-1.220	2.891	62.5
5234.62.....	-2.270	3.221	7.9
Co I			
3894.07.....	0.100	1.049	49.8
3995.31.....	-0.220	0.923	36.0
4092.39.....	-0.940	0.923	19.5
4121.32.....	-0.320	0.923	50.4
Ni I			
3597.70.....	-1.115	0.212	100.6
3612.74.....	-1.423	0.275	70.8
3619.39.....	0.020	0.423	105.3
3775.57.....	-1.408	0.423	59.5
5476.91.....	-0.890	1.826	25.9
Zn I			
4722.15.....	-0.390	4.030	<7
4810.53.....	-0.170	4.080	<7
Sr II			
4077.71.....	0.150	0.000	106.4
Ba II			
4554.03.....	0.163	0.000	85.4
4934.09.....	-0.160	0.000	76.2
5853.67.....	-1.020	0.604	5.9
6141.70.....	-0.070	0.704	30.5

NOTE.—Table 2 is also available in machine-readable form in the electronic edition of the *Astrophysical Journal*.

<sup>a</sup> The “ $\chi$ ” indicates the lines measured but excluded from the abundance analysis. The “s” means the equivalent widths estimated from the spectrum synthesis.

The O I triplet lines at 7770–7776 Å are also clearly detected in CS 29498-043. Figure 2 shows the observed and synthetic spectra for this wavelength range. We note that the observed spectrum in this wavelength range is, unfortunately, affected by fringes due to interference occurring at the surface of the CCD (Noguchi et al. 2002). However, our equivalent widths agree well with those measured by Israelian et al. (2004b) for their Keck High Resolution Echelle Spectrometer (HIRES) spectrum. The oxygen abundance derived from the triplet is 0.47 dex higher than that obtained from the forbidden line (Table 3). However, it should also be noted that the triplet lines are known to be significantly affected by non-LTE (NLTE) effects. Takeda (2003) estimated the NLTE correction for the oxygen abundance derived from the triplet lines to be about -0.1 dex for giants with  $T_{\text{eff}} = 4500$  K. This correction reduces the discrepancy between the oxygen abundances from

the triplet and forbidden lines to about 0.4 dex. Similar discrepancies have also been found in other very metal-poor ( $[\text{Fe}/\text{H}] < -2$ ) stars studied in detail by Takeda (2003). Hence, we do not pursue the origin of this problem further. We note that the discrepancy is larger ( $\sim 0.6$  dex, after NLTE correction) if the lower effective temperature (4400 K) is adopted, since the strengths of the high-excitation triplet lines are quite sensitive to temperature. We adopt the oxygen abundance derived from the forbidden line in the following discussion, because the result is insensitive to the temperature and NLTE corrections.

Israelian et al. (2004a) recently reported a large O overabundance for CS 29498-043 from an analysis of the O I triplet ( $[\text{O}/\text{Fe}] = +3.12$ ), adopting  $T_{\text{eff}} = 4300$  K. The oxygen abundance derived by our LTE analysis for the triplet lines adopting their atmospheric parameters is  $[\text{O}/\text{Fe}] = +3.36$ . They reported the NLTE correction for the oxygen abundance derived from the triplet lines to -0.18 dex for this object; after applying this correction, our results agree very well with theirs.

In addition, Israelian et al. (2004b) also reported the oxygen abundance from the forbidden line that is about 0.5 dex lower than that from the triplet line (the discrepancy is about 0.8 dex after the NLTE correction is applied). This large discrepancy, compared with that found in our above analysis for  $T_{\text{eff}} = 4600$  K (0.4 dex), is likely due to the low assumed effective temperature (4300 K). Israelian et al. (2004a, 2004b) have also detected the O I triplet in the extremely metal-poor star CS 22949-037, which also exhibits similar overabundances in C, N, O, and the  $\alpha$ -elements as in CS 29498-043. They reported an even more significant discrepancy (1.2 dex) between the oxygen abundances derived from the triplet and the forbidden line (Depagne et al. 2002) for CS 22949-037. Given the large discrepancy of oxygen abundances in this object, and also in CS 29498-043, further detailed discussion of O abundances in these objects is difficult. However, it remains clear that the O overabundances are remarkable in these two stars.

### 3.2. Other Elements

A standard analysis using model atmospheres was performed for the measured equivalent widths for most of the other detectable elements, while a spectrum synthesis technique was applied for the C<sub>2</sub> and CN molecular bands and the Al and Mn lines that exhibit contamination from CH molecular lines. The analysis technique and molecular line data are the same as those reported in Aoki et al. (2002a, 2002b). An exception is that the effect of hyperfine splitting is included in the analysis of Mn and Co lines, using the line list of McWilliam et al. (1995) and Pickering (1996), respectively, in the present work.

The results are listed in Table 3. The abundances of the species Co and Ni, which were not detected in the previous spectrum, are reported here for the first time. We searched for MgH  $A-X$  lines in the region 5100–5200 Å but found no clear feature of this molecule. Since the strength of the strongest MgH lines expected for the Mg abundance in Table 3 is about 1 mÅ, spectra with higher quality are required to measure the MgH features.

Random abundance errors in the analysis are estimated from the standard deviation of the abundances derived from individual lines for each species. These values are sometimes unrealistically small, however, when only a few lines are

TABLE 3  
ABUNDANCE RESULTS FOR CS 29498-043

Element (1)	[X/Fe] (2)	log $\epsilon_X$ (3)	$n$ (4)	$\sigma$ (5)	[X/Fe] <sup>a</sup> <sub>4400</sub> (6)	[X/Fe] <sup>b</sup> <sub>103</sub> (7)
<sup>12</sup> C (C <sub>2</sub> ).....	+2.09	7.10	syn	0.29	+2.30	+2.65
N (CN).....	+2.27	6.70	syn	0.40	+2.48	+2.43
O ([O I] 6300).....	+2.43	7.63	1 (syn)	0.11	+2.38	+2.38
O (triplet).....	+2.90	8.10	3 (syn)	0.34	+3.11	+3.36
Na I.....	+1.47	4.25	2	0.38	+1.50	+0.83
Mg I.....	+1.75	5.79	4	0.25	+1.91	+1.46
Al I.....	+0.27:	3.20:	1 (syn)	0.38	+0.32:	-0.15:
Si I.....	+0.82	4.84	1	0.14	+0.90	+0.55
Ca I.....	+0.16	2.97	3	0.16	+0.25	-0.17
Sc II.....	-0.03	-0.47	1	0.34	-0.04	-0.08
Ti I.....	+0.22	1.62	3	0.11	+0.16	-0.32
Ti II.....	+0.38	1.78	9	0.32	+0.39	+0.38
Cr I.....	-0.38	1.77	2	0.10	-0.38	-0.83
Mn I.....	-1.09	0.90	2 (syn)	0.21	-0.56	-1.05
Fe I ([Fe/H]).....	-3.54	3.96	65	0.28	-3.75	-3.94
Fe II ([Fe/H]).....	-3.53	3.97	6	0.34	-3.71	-3.42
Co I.....	+0.06	1.43	4	0.16	+0.00	-0.42
Ni I.....	-0.36	2.35	5	0.29	-0.35	-0.81
Zn I.....	<+0.5	<1.6	2		<+0.5	<+0.9
Sr II.....	-0.47	-1.09	1	0.31	-0.48	-0.48
Ba II.....	-0.46	-1.78	4	0.20	-0.52	-0.58

<sup>a</sup> Abundance results derived for  $T_{\text{eff}} = 4400$  K.

<sup>b</sup> Abundance results derived for the stellar parameters adopted by Israelian et al. (2004a, 2004b).

detected. For this reason, we adopted the larger of (1) the value for the listed species and (2) that for Fe I (0.09 dex) as estimates of the random errors. Errors arising from uncertainties of the atmospheric parameters were evaluated using  $\sigma(T_{\text{eff}}) = 200$  K,  $\sigma(\log g) = 0.5$ , and  $\sigma(v_{\text{turb}}) = 0.5$  km s<sup>-1</sup>. Finally, we derived the total uncertainty by adding in quadrature the individual errors and list them in Table 3.

NLTE effects on our abundance analysis are estimated from the study of metal-poor giants by Gratton et al. (1999). They derived the abundance corrections ( $[X/H]_{\text{NLTE}} - [X/H]_{\text{LTE}}$ ) for Fe (derived from Fe I lines), Na (from the D lines), and Mg to be typically +0.1, +0.0, and +0.2 dex, respectively, for

stars with  $T_{\text{eff}} = 4000\text{--}5000$  K and  $\log g = 1.5$ . The correction for Fe abundance propagates to a change of estimated surface gravity, which is determined from the ionization equilibrium between Fe I and Fe II, by about 0.3 dex. Although this correction will make a systematic change of the abundance results, the effect is still within the uncertainties estimated above.

#### 4. DISCUSSION AND CONCLUDING REMARKS

Recent studies of O abundances in very metal-poor stars, within the framework of one-dimensional model atmospheres, have revealed the presence of a possible increase of O/Fe

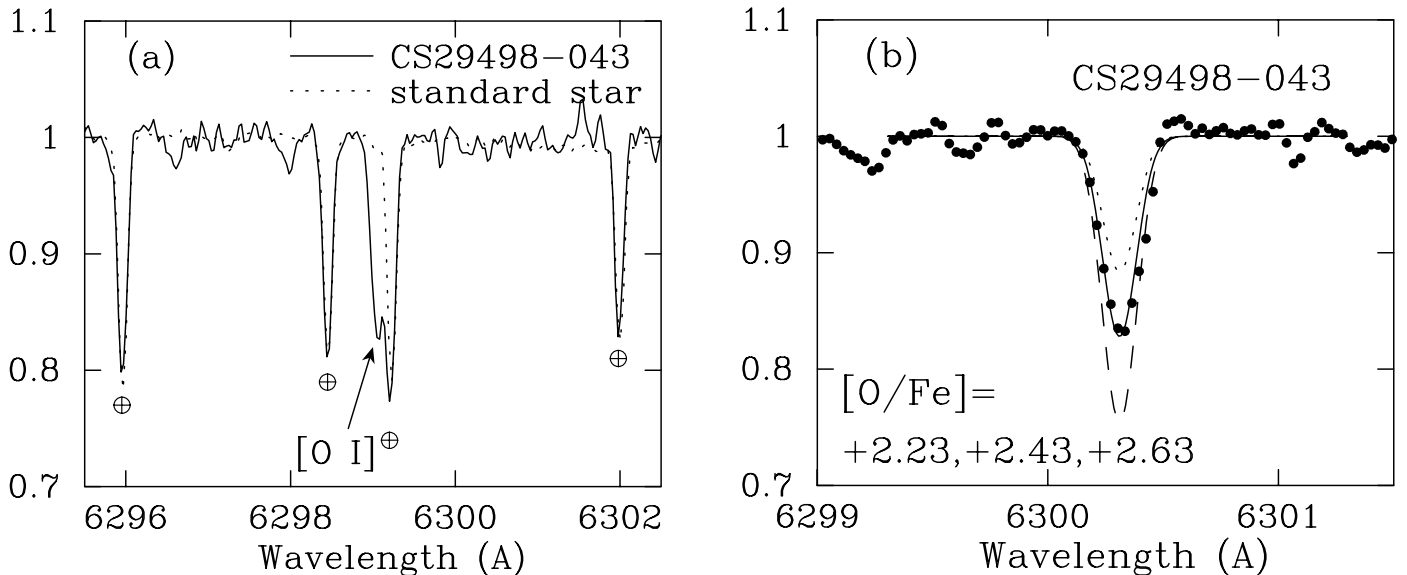


FIG. 1.—(a) Comparison of the spectra of CS 29498-043 and HD 178840 (standard star). Doppler shifts in the spectra are not corrected for. The telluric absorption lines are indicated by crossed circles. (b) Spectrum of CS 29498-043, corrected for the Doppler shift and telluric lines (filled circles). Synthetic spectra assuming  $[O/Fe] = 2.23, 2.43, \text{ and } 2.63$  are shown by dotted, solid, and dashed lines, respectively.

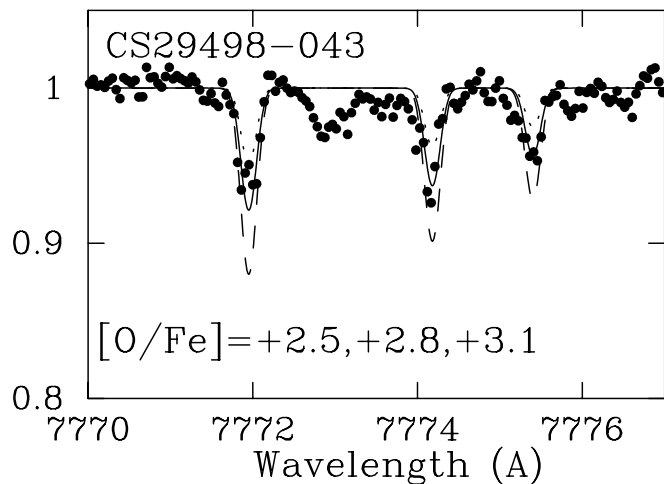


FIG. 2.—Same as Fig. 1*b*, but for the O I triplet lines.

ratios with decreasing metallicity in the range  $[\text{Fe}/\text{H}] < -2$ . Figure 3 shows  $[\text{O}/\text{Fe}]$  as a function of  $[\text{Fe}/\text{H}]$  for our object and for other stars described in the literature (Israelian et al. 2001; Nissen et al. 2002; Cayrel et al. 2004; Bessell et al. 2004). The filled symbols show the  $[\text{O}/\text{Fe}]$  values determined from the [O I] line, while open symbols indicate those obtained from either the triplet lines or OH molecular lines. A discrepancy between the results from the different indicators is seen, as discussed in § 3.1. However, the O overabundance of CS 29498-043, as well as that of CS 22949-037 (Depagne et al. 2002), is unusually high, compared with the other very metal-poor stars ( $[\text{O}/\text{Fe}] \lesssim +1.0$ ). The  $[\text{O}/\text{Fe}]$  of the most iron-deficient star presently known, HE 0107-5240 ( $[\text{Fe}/\text{H}] = -5.3$ ; Christlieb et al. 2002, 2004), is also as high as that found in these two stars (Bessell et al. 2004). We note that even though three of the four objects with  $[\text{Fe}/\text{H}] < -3.5$  have  $[\text{O}/\text{Fe}] \gtrsim +2.0$ , there are stars in this metallicity range in which oxygen lines are *not* detected and hence whose oxygen abundances are not as high as that in these three stars. Although it remains possible that  $[\text{O}/\text{Fe}]$  values continuously increase with decreasing  $[\text{Fe}/\text{H}]$  for stars with  $[\text{Fe}/\text{H}] < -3$ ,

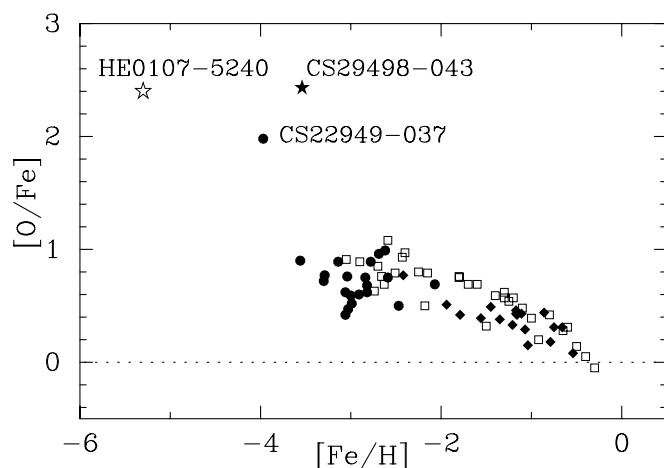


FIG. 3.— $[\text{O}/\text{Fe}]$  as a function of  $[\text{Fe}/\text{H}]$  for CS 29498-043 (filled star, this work) and others in literature: open squares: Israelian et al. (2001); filled diamonds: Nissen et al. (2002); filled circles: Cayrel et al. (2004); and open star: Bessell et al. (2004). The filled symbols show the  $[\text{O}/\text{Fe}]$  values from the [O I] line, while open symbols show those from triplet lines or OH molecular lines.

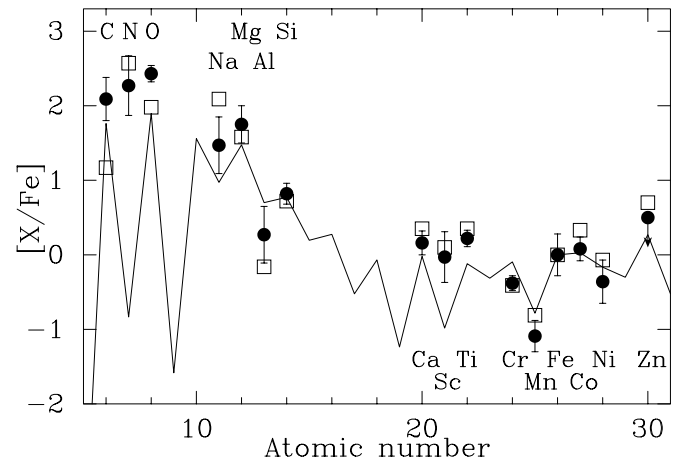


FIG. 4.—Elemental abundance patterns, as a function of atomic number, of CS 29498-043 (filled circles; this work) and CS 22949-037 (open squares; Depagne et al. 2002). The solid line shows an abundance pattern predicted from the Umeda & Nomoto (2003) supernova model for a  $30 M_{\odot}$  star with  $[\text{Fe}/\text{H}] = -4.0$  and the explosion energy of  $5 \times 10^{52}$  ergs, assuming the mixing region of  $M_r = 2.44$ – $12.6 M_{\odot}$  and the matter ejection factor of  $f = 0.004$  (Umeda & Nomoto 2004).

the unusually high oxygen abundances in the above three stars are more likely to arise from a different nucleosynthesis history than that pertaining to other metal-deficient stars.

Figure 4 shows the relative elemental abundances ( $[\text{X}/\text{Fe}]$ ) as a function of atomic number for CS 29498-043 and CS 22949-037. The similarity of the abundance patterns between these two stars is remarkable. The present analysis for the new spectrum of CS 29498-043 confirms the similarity for O and Na, which show large overabundances in both stars. The  $[\text{O}/\text{Fe}]$  value of CS 29498-043 is higher, by 0.36 dex, than that of CS 22949-037, if the same solar O abundance is adopted. However, we do yet not insist on a real difference of the O abundances between the two stars, taking account of the uncertainty in the O abundance determination (as seen, e.g., in the discrepancy in the results between the [O I] line[s] and the O triplet). Recall that for the present analysis, the O abundances in both objects were determined from the [O I] 6300 Å line.

The solid line in Figure 4 shows the abundance ratios predicted by the supernova model of Umeda & Nomoto (2003) for a  $30 M_{\odot}$  star, assuming substantial mixing and fallback (Umeda & Nomoto 2004). The large overabundances of C, O, Mg, and Si relative to iron peak elements are well reproduced by this model. The large overabundance of N in these stars could be associated with the operation of the CN cycle during their evolution on the red giant branch (Depagne et al. 2002). Note as well that the Co/Fe and Ni/Fe ratios of CS 29498-043 might be slightly lower than those of CS 22949-037. The upper limit on the Zn abundance of CS 29498-043 is also lower than the Zn abundance of the other object. In the Umeda & Nomoto (2004) models, lower Co and Zn abundance ratios indicate a smaller explosion energy and/or more effective mixing. More accurate estimates of the abundance ratios of these elements in the present objects, as well as for other similar stars that might be found in the future, are desirable to better constrain the parameters of the present explosion models.

Finally, we would like to consider the metallicity of these objects and their extremely low iron abundances. We here define the metallicity by the *total abundance* of C, N, O, Mg,

Si, and Fe, i.e.,  $[A/H] = [(C + N + O + Mg + Si + Fe)/H]$ . The metallicities of CS 29498-043 and CS 22949-037, using this definition, are  $[A/H] = -1.26$  and  $-2.00$ , respectively. Oxygen is the most important contributor to the metallicity in these stars (60%–70% of the metallic species). When we adopt the above definition of metallicity, these three objects might be regarded as *extremely iron-deficient stars* rather than *extremely metal-poor stars*.

The metallicity of the most iron-poor ( $[Fe/H] = -5.3$ ) star HE 0107–5240 (Christlieb et al. 2002, 2004) is  $[A/H] = -1.77$ , using this definition, adopting  $[O/Fe] = +2.4$  (Bessell et al. 2004), and assuming  $[Si/Fe] = 0.0$ . In this case, however, the dominant contributor to the metallicity is carbon (about 95%). The abundance pattern of this object can also be explained by supernova models by Umeda & Nomoto (2003), assuming a larger mixing region and a smaller matter ejection factor. Although this object shows no clear overabundance of  $\alpha$ -elements, the origin of its peculiar abundance pattern may be related to those of CS 29498-043 and CS 22949-037.

The extremely iron-deficient ( $[Fe/H] < -3.5$ ) stars found in previous studies (Norris et al. 2001; Carretta et al. 2002; François et al. 2003) generally *do not exhibit* large excesses of lighter elements, except for CS 22949-037 (Norris et al. 2001). These stars can be regarded as extreme cases of metal-deficient stars with higher iron abundance ( $-3.5 < [Fe/H] \leq -2.5$ ), which would form from interstellar matter polluted by first-generation supernovae. Their extremely low metallicity suggests high explosion energies of the supernovae that provided metals and induced the formation of second-generation stars (e.g., Cioffi et al. 1988). Hence, the formation mechanism of the above three iron-deficient stars with excesses of C and O may be quite different from the other iron-deficient stars. Even though their total atmospheric metallicities are rather high ( $[A/H] \gtrsim -2$ ), these three stars are also expected

to be produced from material polluted by first-generation supernovae because of their peculiar abundance patterns. However, the extremely low iron abundances of these objects might be regarded as resulting from the particular yields of their progenitors, rather than from mixing processes within the interstellar matter from which they were formed. The relatively high total metallicity of these objects may indicate low explosion energies of the supernovae that induced the formation of these objects.

If the species C and O were present in the interstellar matter of the birth clouds of these objects, they would supply important cooling sources, in particular for HE 0107–5240; hence, their overabundances may help explain the possibility of low-mass star formation in the early Galaxy, as suggested by Umeda & Nomoto (2003) (see also Bromm & Loeb 2003). This may also explain the existence of the plethora of C-rich objects among extremely iron-deficient stars (Norris et al. 1997; Beers 1999; Rossi et al. 1999). Further abundance studies of stars with extremely low iron abundances are indispensable to establish the proper classification of these stars and to understand the formation mechanism(s) of early-generation stars in our Galaxy.

We are grateful to F.-J. Zickgraf for carrying out the photometric observations (*R* and *I* band), and to B. Marsteller for the speedy data reduction, which provided confirmatory information for our temperature estimate of CS 29498-043. J. E. N. acknowledges support from grant DP0342613 of the Australian Research Council. T. C. B. acknowledges partial support from grants AST 00-98508 and AST 00-98549 awarded by the US National Science Foundation. N. C. is grateful to the American Astronomical Society for financial support through a Chretien International Research Grant.

#### REFERENCES

- Allende Prieto, C., Lambert, D. L., & Asplund, M. 2001, *ApJ*, 556, L63  
 Alonso, A., Arribas, S., & Martínez-Roger, C. 1999, *A&AS*, 140, 261  
 Aoki, W., Norris, J. E., Ryan, S. G., Beers, T. C., & Ando, H. 2002a, *ApJ*, 576, L141  
 ———. 2002b, *PASJ*, 54, 933  
 Beers, T. C. 1999, in *ASP Conf. Ser. 165, Third Stromlo Symposium: The Galactic Halo*, ed. B. K. Gibson, T. S. Axelrod, & M. E. Putman (San Francisco: ASP), 202  
 Bessell, M. S., Christlieb, N., & Gustafsson, B. 2004, *ApJ*, submitted (astro-ph/0401450)  
 Bromm, V., & Loeb, A. 2003, *Nature*, 425, 812  
 Carretta, E., Gratton, R., Cohen, J. G., Beers, T. C., & Christlieb, N. 2002, *AJ*, 124, 481  
 Cayrel, R., et al. 2004, *A&A*, 416, 1117  
 Christlieb, N., Gustafsson, B., Korn, A. J., Barklem, P. S., Beers, T. C., Bessell, M. S., Karlsson, T., & Mizuno-Wiedner, M. 2004, *ApJ*, 603, 708  
 Christlieb, N., et al. 2002, *Nature*, 419, 904  
 Cioffi, D. F., McKee, C. F., & Bertschinger, E. 1988, *ApJ*, 334, 252  
 Depagne, E., et al. 2002, *A&A*, 390, 187  
 François, P., et al. 2003, *A&A*, 403, 1105  
 Gratton, R. G., Carretta, E., Eriksson, K., & Gustafsson, B. 1999, *A&A*, 350, 955  
 Israelian, G., Rebolo, R., García López, R. J., Bonifacio, P., Molaro, P., Basri, G., & Shchukina, N. 2001, *ApJ*, 551, 833  
 Israelian, G., Shchukina, N., Rebolo, R., Basri, G., & González Hernández, J. I. 2004a, in *Origin and Evolution of the Elements*, ed. A. McWilliam & M. Rauch (Pasadena: Carnegie Obs.), <http://www.ociv.edu/ociv/symposia/series/symposium4/proceedings.html>
- Israelian, G., Shchukina, N., Rebolo, R., Basri, G., González Hernández, J. I., & Kajino, T. 2004b, *A&A*, in press  
 Kurucz, R. L. 1993, Kurucz CD-ROM 13, ATLAS9 Stellar Atmospheres Programs and 2 km/s Grid (Cambridge: SAO)  
 McWilliam, A., Preston, G. W., Sneden, C., & Searle, L. 1995, *AJ*, 109, 2757  
 Nissen, P. E., Primas, F., Asplund, M., & Lambert, D. L. 2002, *A&A*, 390, 235  
 Noguchi, K., et al. 2002, *PASJ*, 54, 855  
 Norris, J. E., Ryan, S. G., & Beers, T. C. 1997, *ApJ*, 488, 350  
 ———. 1999, *ApJS*, 123, 639  
 ———. 2001, *ApJ*, 561, 1034  
 Pickering, J. C. 1996, *ApJS*, 107, 811  
 Rossi, S., Beers, T. C., & Sneden, C. 1999, in *ASP Conf. Ser. 165, Third Stromlo Symposium: The Galactic Halo*, ed. B. K. Gibson, T. S. Axelrod, & M. E. Putman (San Francisco: ASP), 264  
 Ryan, S. G., Norris, J. E., & Beers, T. C. 1996, *ApJ*, 471, 254  
 Schlegel, D. J., Finkbeiner, D. P., & Davis, M. 1998, *ApJ*, 500, 525  
 Skrutskie, M. F., et al. 1997, in *The Impact of Large Scale Near-IR Sky Surveys*, ed. F. Garzon, N. Epchtein, A. Omont, B. Burton, & P. Persi (Dordrecht: Kluwer), 187  
 Takeda, Y. 2003, *A&A*, 402, 343  
 Tsujimoto, T., & Shigeyama, T. 2003, *ApJ*, 584, L87  
 Umeda, H., & Nomoto, K. 2003, *Nature*, 422, 871  
 ———. 2004, *ApJ*, submitted (astro-ph/0308029)